Active Site Modifications in a Double Mutant of Liver Alcohol Dehydrogenase: Structural Studies of Two Enzyme−Ligand Complexes[†,‡]

Thomas D. Colby,[§] Brian J. Bahnson,[||,⊥] Jodie K. Chin,[||] Judith P. Klinman,*[,||,#] and Barry M. Goldstein*[,§]

Department of Biochemistry and Biophysics, University of Rochester Medical Center, Rochester, New York 14642, and Departments of Chemistry and of Molecular and Cell Biology, University of California, Berkeley, California 94720

Received December 30, 1997; Revised Manuscript Received April 13, 1998

ABSTRACT: The oxidation of alcohol to aldehyde by horse liver alcohol dehydrogenase (LADH) requires the transfer of a hydride ion from the alcohol substrate to the cofactor nicotinamide adenine dinucleotide (NAD). A quantum mechanical tunneling contribution to this hydride transfer step has been demonstrated in a number of LADH mutants designed to enhance or diminish this effect [Bahnson, B. J., et al. (1997) *Proc. Natl. Acad. Sci. U.S.A. 94*, 12797−12802]. The active site double mutant Phe[93] → Trp/Val[203] → Ala shows a 75-fold reduction in catalytic efficiency relative to that of the native enzyme, and reduced tunneling relative to that of either single mutant. We present here two crystal structures of the double mutant: a 2.0 Å complex with NAD and the substrate analogue trifluoroethanol and a 2.6 Å complex with the isosteric NAD analogue CPAD and ethanol. Changes at the active site observed in both complexes are consistent with reduced activity and tunneling. The NAD−trifluoroethanol complex crystallizes in the closed conformation characteristic of the active enzyme. However, the NAD nicotinamide ring rotates away from the substrate, toward the space vacated by replacement of Val[203] with the smaller alanine. Replacement of Phe[93] with the larger tryptophan also produces unfavorable steric contacts with the nicotinamide carboxamide group, potentially destabilizing hydrogen bonds required to maintain the closed conformation. These contacts are relieved in the second complex by rotation of the CPAD pyridine ring into an unusual syn orientation. The resulting loss of the carboxamide hydrogen bonds produces an open conformation characteristic of the apoenzyme.

Horse liver alcohol dehydrogenase (LADH)[1] catalyzes the first and rate-limiting step in alcohol metabolism, the oxidation of alcohol to aldehyde. This reaction requires the transfer of a hydride ion from the alcohol substrate to the cofactor NAD. Despite the fact that LADH is one of the enzymatic systems most extensively studied to date, the mechanism of the hydride transfer step remains an area of active investigation. Studies presented here and elsewhere (*1*) suggest a link between active site structure, enzyme conformation, and the catalytic hydride transfer step.

LADH is a dimeric protein with each 40 kDa monomer consisting of a catalytic and a coenzyme binding domain. The active site, located at the base of the cleft between the two domains, contains a tetracoordinate zinc cation. Three of the zinc ligands are supplied by the enzyme. In the "open" form of the apoenzyme, the active site is accessible to solvent and the fourth zinc ligand is occupied by water. When cofactor binds, it induces a transformation to a "closed" form of the enzyme. This isomerization step requires a rotation of the catalytic domain relative to the coenzyme binding domain, resulting in a narrowing of the interdomain cleft and a more hydrophobic environment at the active site (*2*, *3*). This rearrangement facilitates displacement of water by alcohol as the fourth coordination ligand of the catalytic zinc and places the zinc-bound substrate close to the C4 position of the cofactor's nicotinamide ring. The isomerization step is required for hydride transfer (*4*, *5*).

Once the enzyme adopts the closed form, the substrate and cofactor are sufficiently close to allow direct transfer of a hydride ion from the alcohol secondary carbon to the C4 position of the nicotinamide ring. A quantum mechanical tunneling contribution to this hydride transfer step has been demonstrated (*6*), and kinetic isotope effects consistent with tunneling have been observed in a number of LADH mutants (*1*, *7*).

The design of LADH mutants for studying tunneling has been based on two hypotheses. In native LADH, the release of the product is partially rate-limiting (*5*), masking detection of a possible tunneling effect. Mutants were designed to increase the off rate of product aldehyde to make the hydride

[†] Supported in part by NSF Grant MCB-9514126 (J.P.K.), an NIGMS postdoctoral fellowship training grant (B.J.B.), and an NIH Molecular Biophysics training grant (J.K.C.).

[‡] Crystallographic coordinates have been deposited in the Brookhaven Protein Data Bank under file names 1A71 and 1A72 for the NAD and CPAD mutant complexes, respectively.

* To whom correspondence should be addressed. E-mail: bmg@bphvax.biophysics.rochester.edu.

[§] University of Rochester Medical Center.

[||] Department of Chemistry, University of California.

[⊥] Current address: Rosenstiel Center, Brandeis University, Waltham, MA 02254.

[#] Department of Molecular and Cell Biology, University of California.

[1] Abbreviations: LADH, horse liver alcohol dehydrogenase; F93W, Phe[93] → Trp mutation; V203A, Val[203] → Ala mutation; F93W/V203A, Phe[93] → Trp/Val[203] → Ala double mutant; NAD, nicotinamide adenine dinucleotide; CPAD, 5-β-D-ribofuranosylpicolinamide adenine dinucleotide.

S0006-2960(97)03184-X CCC: $15.00
Published on Web 06/11/1998

transfer step more rate-limiting, thereby unmasking the tunneling effect. The product off rate was increased by shrinking the size of the substrate binding pocket through the addition of steric bulk. Bulk was introduced by mutation of Phe^{93} to tryptophan, which adds an additional hydrophobic ring at the base of the binding pocket. Kinetics of this F93W mutant revealed an isotope effect deviating from the semiclassical range in the direction expected from tunneling (*7*).

A second motivation for mutant design exploits the hypothesis that active site geometry has evolved to optimize the tunneling component of the hydride transfer process (*1*). Thermal fluctuations in protein conformation can significantly enhance tunneling by shortening the distance between donor and acceptor atoms along the reaction coordinate (*8*, *9*). In LADH, the active site is sandwiched between the catalytic and coenzyme-binding domains. In the closed conformation, thermally induced interdomain motion could compress the distance between the nicotinamide ring and substrate. The back face of the nicotinamide ring makes hydrophobic contact with the highly conserved residue Val^{203}, which might be expected to influence the hydride transfer distance between donor and acceptor. As predicted, mutation of Val^{203} to less bulky side chains results in reduced rates and changes in isotope effects consistent with reduced tunneling (*1*).

To test the structural assumptions behind these mutations, we examined crystal structures of ternary complexes of the LADH active site single mutants F93W and V203A (*1*). The single F93W mutant displays isotope effects characteristic of a significant tunneling contribution, with a catalytic efficiency comparable to that of the wild type enzyme (*7*). The relative conformation of the cofactor and trifluoroethanol substrate analogue in the F93W mutant structure does, in fact, approximate that of an active ternary complex in the closed conformation (*1*). In contrast, the V203A mutant shows reduced tunneling and an almost 40-fold reduction in catalytic efficiency relative to that of F93W (*1*). The crystal structure of the V203A mutant shows a compromised catalytic site geometry, with the NAD nicotinamide ring rotating away from the substrate, toward the gap left by replacement of the adjacent bulky valine at position 203 with the smaller alanine (*1*). This increases the distance for hydride transfer in the ground state structure.

Given the contrasting kinetic and structural properties of the two single mutants, examining the double LADH mutant F93W/V203A was of particular interest. The V203A/F93W double mutant shows a 75-fold reduction in catalytic efficiency relative to that of the native enzyme, and reduced tunneling relative to that of either single mutant (*1*). We present here the structures of two complexes of the double mutant F93W/V203A. One structure contains the normal cofactor NAD and the substrate analogue trifluoroethanol. These ligands are the same as those used in the single mutant structures (*1*). The second double mutant complex was crystallized with ethanol as the substrate and the isosteric NAD analogue, CPAD, as a cofactor analogue. CPAD contains a neutral pyridine ring in place of the nicotinamide ring (*10*).

Comparison of the four mutant complexes examined to date suggests that measured differences in catalytic efficiency and hydride tunneling can be interpreted, in part, by observed structural differences in the ground state active site complexes. Comparison of these structures also suggests that differences in dynamic behavior of the protein may play a contributing role in modulating tunneling.

Table 1: Data Collection and Refinement Statistics for the F93W/V203A LADH Complexes

	NAD−trifluoroethanol	CPAD
space group	*P*1	$C222_1$
a (Å)	50.6	55.5
b (Å)	44.1	74.2
c (Å)	92.6	179.2
α (deg)	103.0	90.0
β (deg)	87.9	90.0
γ (deg)	70.7	90.0
monomers/asymmetric unit	2	1
total reflections measured	77 199	16 939
unique reflections [$I_o/\sigma(I) \geq 1.0$]	38 046	10 388
R_{merge} (%)	7.1	7.8
maximum resolution, d_{min} (Å)	2.0	2.6
completeness to d_{min} [%, $I/\sigma(I) > 1$]	77.1	76.9
completeness at d_{min} [%, $I/\sigma(I) > 1$]	42.3	43.0
$\langle I/\sigma(I)\rangle$ (all data)	7.5	6.0
$\langle I/\sigma(I)\rangle$ (last shell)	2.0	2.0
data range used in refinement (Å)	10.0−2.0	8.0−2.6
R (%)	19.9	17.6
R_{free} (%)	28.8	*a*
rms deviations		
bond lengths (Å)	0.008	0.013
bond angles (deg)	1.7	2.0
dihedral angles (deg)	24.0	25.3
improper torsions (deg)	1.4	1.6
no. of waters	179	83

[a] Final R_{free} not calculated (see the text).

EXPERIMENTAL PROCEDURES

F93W/V203A LADH−NAD−Trifluoroethanol Complex. The F93W/V203A double mutant was expressed and purified as described (*7*). Protein was dialyzed against 50 mM Tris buffer (pH 8.4 at 4 °C) and concentrated to 13 mg/mL in three washes using Centricon 50 centrifugal concentrators (Amicon, Beverly, MA). A 10-fold molar excess of NAD (Boehringer Mannheim, Indianapolis, IN) was added to the concentrated protein solution, followed by trifluoroethanol (Aldrich, Milwaukee, WI) and PEG 400 (Fluka, Ronkonkoma, NY) to concentrations of 5 mM and 4% (v/v), respectively. The solution was filtered through a 0.45 μm cellulose acetate filter (Costar, Cambridge, MA). Crystals were grown by vapor diffusion at 4 °C from 4 μL drops equilibrated against wells containing Tris buffer (pH 8.4), 5 mM trifluoroethanol, and 18% PEG 400 (v/v).

Data were obtained from a single loop-mounted crystal washed briefly (≤30 s) in a drop of buffer containing trifluoroethanol, NAD, and 30% PEG 400 and then flash-frozen and maintained at −170 °C in a stream of dry nitrogen gas (*11*). Data were collected using an R-AXIS II area detector with a Cu rotating anode source running at 50 kV and 100 mA. The oscillation method was used, with an exposure time of 40 min per degree per frame, a crystal-to-detector distance of 100 mm, and no 2θ offset. Frames were indexed and reduced, and reflections were scaled, integrated, and averaged using the HKL package (*12*). Crystal data and intensity statistics are given in Table 1.

The F93W/V203A−NAD complex is isomorphous to the 1.8 Å LADH−NADH complex determined by Al-Karadaghi et al. (*13*). The latter served as the initial phasing model for an isomorphous replacement solution using X-PLOR version 3.1 (*14*). The model was subjected to grouped rigid body refinement, with each monomer domain serving as an independent group. The resulting model was used to generate initial $F_o - F_c$ and $2F_o - F_c$ maps with mutated residues, inhibitor, and cofactor omitted. The tryptophan at position 93 and cofactor were manually fit to the resulting electron density. Initial maps clearly indicated 2′-endo sugar puckers for both cofactor moieties. Puckers were restrained through subsequent stages of refinement. Harmonic restraints were also applied to the cofactor adenine and nicotinamide moieties to maintain planarity. Refinement was carried out with parchcsdx.pro and tophcsdx.pro parameter and topology files (*14*, *15*) and the X-PLOR NAD parameters. Map display and model building were carried out with the program CHAIN (*16*).

The initial complex was subjected to 100 steps of constrained conjugate gradient refinement, followed by 10 steps of overall *B*-factor refinement and 20 steps of individual *B*-factor refinement. R_{free} and R were monitored throughout (*17*). The trifluoroethanol substrate analogue was manually fitted at this stage and again subjected to conjugate gradient and *B*-factor refinement. Simulated annealing using the slow-cooling strategy (*18*) produced no improvement in the model, resulting in an increased R_{free} and no change in active site geometry. Thus, this stage of refinement was omitted. Maps calculated at this stage were used to place 179 solvent molecules on the basis of the following criteria: a peak height of at least 2.0σ on an $F_o - F_c$ map, 1.0σ on a $2F_o - F_c$ map, and reasonable intermolecular contacts. Manual refitting of the ligand cofactor and the coordination geometry of the catalytic zinc was performed, and the charge on the zinc, its ligands, and the substrate were switched off. The van der Waals radius of the zinc was set to 0.65 Å, and harmonic constraints were applied to the four catalytic zinc coordination distances in each monomer. This model was subjected to a third round of conjugate gradient and *B*-factor refinement. Conjugate gradient refinement was then repeated with all constraints released. The final model showed reasonable zinc coordination geomety. Refinement statistics are summarized in Table 1.

F93W/V203A LADH−CPAD Complex. Crystals of the LADH mutant F93W/V203A complexed with the inhibitor CPAD (*10*) were obtained as described above, with several modifications. Protein was dialyzed against 50 mM Tris buffer (pH 8.4 at 4 °C) containing 4% (v/v) ethanol, concentrated to 10 mg/mL, and a 10-fold molar excess of CPAD was added to the solution prior to filtration. X-ray grade crystals were obtained by vapor diffusion at 4 °C from 4 μL drops equilibrated against reservoirs containing 50 mM Tris buffer and 11−13% (v/v) ethanol. Crystals were mounted with mother liquor in sealed quartz capillary tubes.

Diffraction data were collected at 3 ± 1 °C on a Xentronics area detector with a Cu rotating anode X-ray source operating at 60 kV and 50 mA. Data were collected using an oscillation width of 0.25°, exposure times of 2−4 min/frame, a crystal-to-detector distance of 16 cm, and a 2θ offset of 20°. Data were processed using XDS software (*19*, *20*). Crystal data and intensity statistics are given in Table 1.

The F93W/V203A LADH−CPAD complex is isomorphous to the open form native apoenzyme (*21*), and the native apomonomer was used as the phasing model. Initial conjugate gradient and *B*-factor refinement proceeded as above. The $2F_o - F_c$ and $F_o - F_c$ omit maps confirmed the mutations and showed density corresponding to the adenine end of the CPAD inhibitor. In this case, the structure was subjected to alternating cycles of simulated annealing and manual model building, as described previously (*22*, *23*). At each stage, omit maps were used to fit successively larger fragments of the CPAD dinucleotide.

Force and topology parameter files for CPAD were based on the X-PLOR NAD files. Parameters for the pyridine end of the CPAD ligand were modified on the basis of ab initio calculations using Gaussian92 (*24*). Harmonic restraints were used to maintain the CPAD adenine ribose in a 2′-endo pucker and the pyridine ribose in a 3′-endo pucker.

The planes of the pyridine ring and its carboxamide substituent were restrained to lie within 30° of each other, with the carboxamide amino group cis to the adjacent pyridine nitrogen. This conformation is favored by ∼10 kcal/mol over the trans carboxamide conformation, as determined by ab initio methods described previously (*25*). Computations suggest that, in this position, a carboxamide amino hydrogen forms strong charge transfer interactions with the pyridine nitrogen. This carboxamide conformation differs by ∼180° from that used for NADH in an analogous LADH−imidazole complex (*26*) (see Results). The carboxamide group in NAD(H) lacks the adjacent nitrogen and shows a 2−4 kcal/mol preference for the trans conformation (*25*).

Cross-validation using an R_{free} test set was insensitive to the conformation at the pyridine end of the CPAD ligand. Prior to complete fitting of the ligand, $R_{free} = 30.3\%$ and $R = 23.7\%$. Due to the limited completeness and resolution of the data, all data were used in subsequent fitting and refinement. SA omit maps were calculated for the region surrounding the cofactor binding site to provide an unbiased check of the CPAD conformation (*27*). Annealing was performed with the CPAD molecule, and all residues within 3 Å of the ligand were omitted. Resulting maps supported the final position of the adenine moiety, the pyrophosphate bridge, the pyridine ribose, and the carboxamide group. However, the electron density for the CPAD pyridine ring was less well defined, suggesting high mobility.

The only side chain that required significant manual manipulation relative to the apoenzyme structure was Arg^{47}, a residue that appears in different positions depending on the complex (*22*, *28*). In our structure, this arginine is rotated away from the inhibitor, as is seen in the structure of the wild type enzyme with the inhibitors βTAD and βSAD (*22*).

Following annealing, 83 ordered solvent molecules were added to the model using the criteria described above. A 4σ peak consistently appeared in $F_o - F_c$ maps in the region of the fourth coordination ligand of the catalytic zinc. This electron density may represent coordinated ethanol, as observed in previous LADH complexes (*23*). Although ethanol was present in the crystallization medium, the resolution was insufficient to orient it in the model. Thus, the zinc ligand was modeled as a single water molecule, although this was insufficient to account for all of the electron

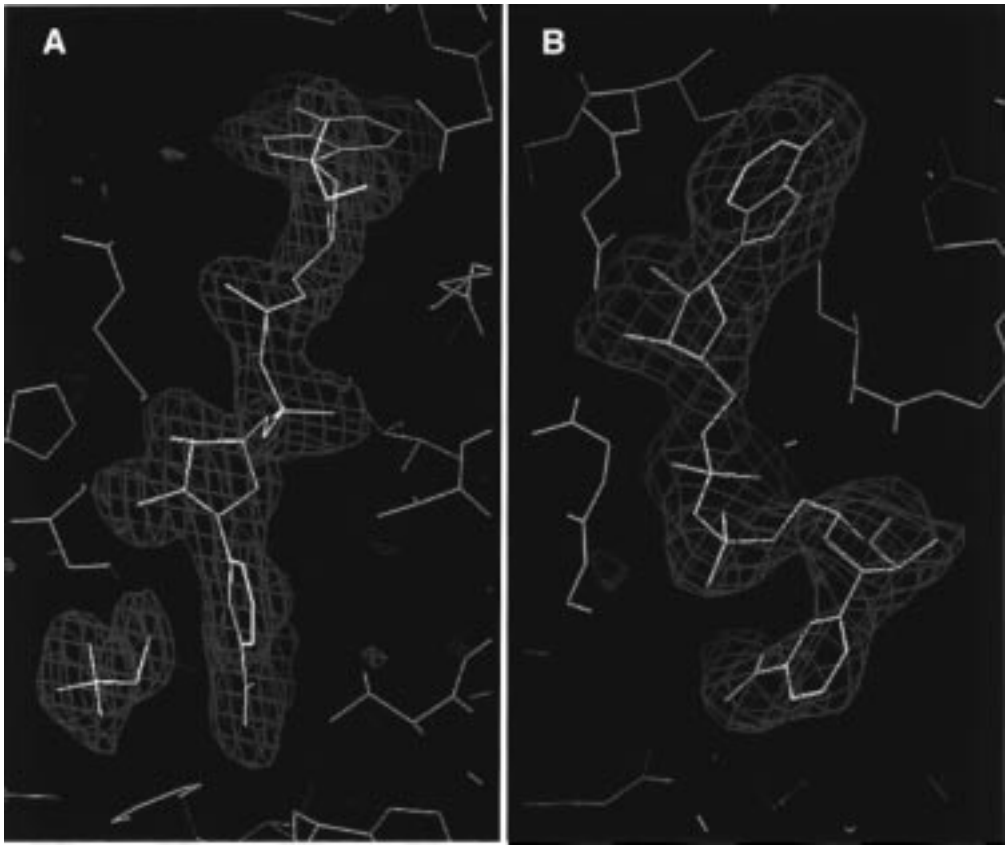

FIGURE 1: $F_o - F_c$ maps of the cofactor binding region of the F93W/V203A LADH mutant complexed with NAD (A) and the NAD analogue CPAD (B). In the NAD complex (A), the density corresponding to the bound trifluoroethanol substrate analogue is also shown. Maps are contoured in red at the 2.5σ (A) and 2.0σ (B) levels. Ligand models and adjacent residues are shown in white.

density in the region. The "substrate" water was refined to a final coordination distance of 1.76 Å.

The final model was subjected to 120 steps of conjugate gradient minimization with all constraints removed. This was followed by 10 steps of overall *B*-factor refinement and 20 steps of individual *B*-factor refinement. Refinement statistics are summarized in Table 1.

Ab Initio Calculations. Ab initio calculations using Gaussian94 (*29*) were performed on model complexes to quantify the effects of the Phe^{93} → Trp substitution on the stability of the ligand carboxamide group hydrogen bonds. Models for the NAD complexes contained a nicotinamide ring with a methyl substituent on the pyridinium nitrogen. Hydrogen bonds between the carboxamide group and the main chain amide proton and carbonyl oxygens of residues 292, 317, and 319 were modeled by a formamide proton and two formaldehyde oxygens, respectively. The side chain of residue 93 was modeled by either a phenyl group with a methyl substituent for the native Phe^{93} or an indole moiety for the Trp^{93} mutation. Groups were placed in the same relative geometries as observed in the native and mutant closed complex crystal structures. The influence of the "side chain" on H-bond stability was determined as follows. Each component of the model (methylnicotinamide ring, formamide and formaldehyde groups, and methyl-substituted phenyl and indole rings) was minimized separately at the HF/6-31G* level (*30*). A single-point energy *E* was then obtained using the BPW91 density functional model with a 6-31G basis set (*30*). This energy was obtained for the entire complex ($E_{complex}$), the nicotinamide ring and formamide and formaldehyde H-bonding groups ($E_{nicotinamide}$), and the phenyl or indole side chain ($E_{side\ chain}$). The change in energy (ΔE) induced by the presence of the side chain is then equal to $E_{complex} - (E_{nicotinamide} + E_{side\ chain})$ (*31*). Calculations for complexes containing the CPAD analogue were performed in the same manner, using a 2-carboxamide, 4-methyl pyridine moiety in place of the methyl-substituted nicotinamide ring.

RESULTS

V203A/F93W−NAD

The ternary complex with the double mutant, NAD, and trifluoroethanol crystallizes in a closed conformation isomorphous to that seen for the single F93W mutant (*1*) and for native complexes with NAD (*13*, *32*−*35*). The rms fit between backbone atoms of the double mutant and the native enzyme in its closed conformation is 0.32 Å. There are two crystallographically independent monomers in the dimeric asymmetric unit. The monomer structure does not display the "hyperclosure" of the catalytic and cofactor binding domains observed in the V203A single mutant (*1*).

The NAD cofactor is bound in an extended conformation in the narrowed cleft between the catalytic and cofactor binding domains (Figure 1A). NAD− and substrate−enzyme interactions are generally similar to those observed in higher-resolution ternary complexes of the native enzyme and are described below (*13*, *33*). However, the F93W/V203A mutations do produce two significant effects on cofactor binding at the active site. As might be expected, deviations from normal substrate and cofactor binding

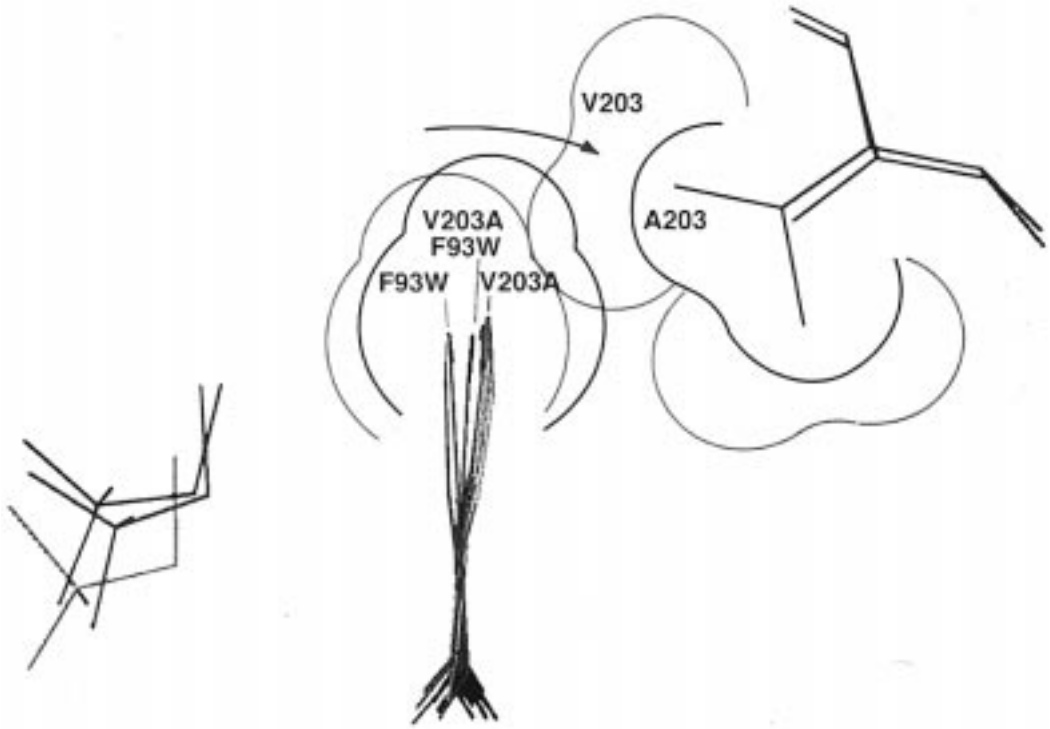

FIGURE 2: Comparison of active site structures of complexes between NAD, trifluoroethanol, and three LADH mutants: F93W (cyan), F93W/V203A (magenta), and V203A (gray). The trifluoroethanol substrate analogue is at left. Overlaps of the two (F93W and F93W/V203A) or four (V203A) crystallographically independent NAD nicotinamide rings are at center, viewed edge-on along the glycosidic bond. The side chain of residue 203 is at right. van der Waals surfaces are drawn for the F93W and F93W/V203A mutants. Nicotinamide overlaps are based on a least-squares alignment of the eight independent cofactor binding domains from the three mutants. The nicotinamide ring in F93W is in van der Waals contact with Val^{203}. In both V203A and F93W/V203A, the nicotinamide ring rotates (curved arrow) to fill the gap left by the substitution with alanine. Further rotation of the rings is prevented by steric contacts with Trp^{93} for F93W/V203A and with Thr^{178} for both mutants (not shown). Displacement of substrate observed in V203A is blocked by the $Phe^{93} \rightarrow Trp$ mutation in F93W and F93W/V203A (Figure 3).

combine features observed in both the F93W and V203A single mutants.

NAD Cofactor Binding and Nicotinamide Ring Rotation. The cofactor nicotinamide ring rotates away from the substrate, into the space left by replacement of Val^{203} with the smaller alanine side chain (Figure 2). The normals to the nicotinamide planes in the two monomers are rotated by an average of 7° toward mutated residue 203, relative to the position observed in both the wild type enzyme and the F93W single mutant (*1*). The center of the ring is also shifted by an average of 0.3 Å toward position 203. Rotation and displacement of the nicotinamide ring compromise the catalytic geometry (Figure 2). The distance between the hydride-donating methylene carbon on the trifluoroethanol substrate analogue and the accepting carbon C4 on the nicotinamide ring is increased by ~0.4 Å relative to that seen in the single F93W mutant (*1*).

This increase in distance is observed in the V203A single mutant as well, albeit to a greater extent (Figure 2). The plane of the nicotinamide ring in the V203A complex shows an average rotation of 10° toward mutated residue 203 (*1*). An equal displacement of the nicotinamide ring in the F93W/V203A double mutant is prevented by close steric contacts between the carboxamide oxygen and the larger tryptophan side chain at position 93 (see below). In both single and double mutants, further rotation of the nicotinamide ring toward Ala^{203} is also prevented by van der Waals contacts with residue Thr^{178}. In the double mutant, reductions in tunneling are likely to arise from several effects, in addition to the increase in distance between the reacting carbons (below).

NAD Cofactor Binding and Carboxamide Interactions. Despite its rotation, the NAD carboxamide oxygen maintains its hydrogen bond with the main chain nitrogen of Phe^{319} and the carboxamide amino group donates hydrogen bonds to the carbonyl oxygens of Val^{292} and Ala^{317} (Figure 3). These cofactor−side chain hydrogen bonds are seen in all closed-form complexes between LADH and either NAD (*13*, *32*−*36*) or isosteric NAD analogues (*23*, *28*). Cofactor analogues which are unable to form these carboxamide−enzyme hydrogen bonds bind in the open conformation, suggesting that these interactions are required to maintain the closed conformation of the complex (*23*, *26*, *32*, *37*). These cofactor−enzyme interactions are potentially destabilized by the F93W mutation.

Interference by the larger Trp^{93} side chain in the double mutant may limit the role of the carboxamide oxygen as a hydrogen bond acceptor from the main chain NH of Phe^{319} (Figure 3). Replacement of Phe^{93} with the bulkier tryptophan side chain causes severe crowding of both the nicotinamide carboxamide group and its amide proton donor (Figure 3). The Trp^{93} Cη2 carbon is 3.1 Å from the nicotinamide carboxamide oxygen, placing the Trp^{93} Cη2 hydrogen within ~2.0 Å of both the carboxamide oxygen and the main chain amide proton donor of residue Phe^{319}. By comparison, the closest proton on Phe^{93} in the native closed complex (attached to Cϵ2) is more than 3 Å from both the carboxamide oxygen and the main chain amide proton. The mutated Trp^{93} side

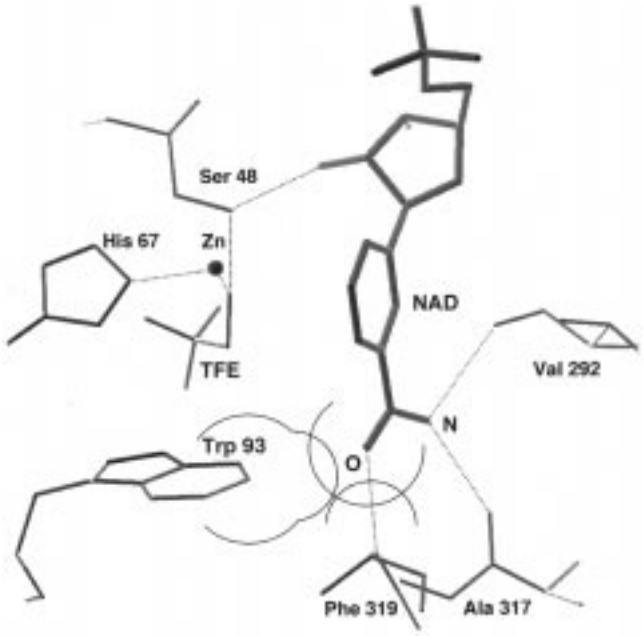

FIGURE 3: Active site resdues and ligands in the closed F93W/V203A−NAD−trifluoroethanol complex. Hydrogen bonds and Zn ligands are shown as dotted lines (only one enzyme−Zn ligand to His^{67} is shown for clarity). van der Waals surfaces are drawn around the nicotinamide carboxamide oxygen, the H-bond donating main chain amino proton of residue 319, and the Cη2−H atoms of mutated residue Trp^{93}. Close steric contacts with Trp^{93} destabilize the three carboxamide hydrogen bonds to residues 317, 319, and 292 required for maintaining the closed conformation of the enzyme.

chain is stabilized in its crowded site by a hydrogen bond between the indole amide proton and the main chain oxygen of Gly^{173}. These interactions are also observed in the F93W single mutant.

Close contacts between aromatic protons and nucleophilic atoms lying within the plane of the conjugated ring are observed in both small molecule (*38*) and protein structures (*39*−*41*). These contacts have been attributed to stabilizing "weakly polar interactions" of electrostatic origin (*38*−*40*). This raises the question of whether the close Trp^{93}−carboxamide contact observed in the F93W mutant is energetically favorable.

To quantitatively evaluate the effects of the F93W mutation on the critical nicotinamide carboxamide hydrogen bonds, ab initio calculations were performed on model native and mutant complexes (see Experimental Procedures). Results indicate that the proximity of the Phe^{93} side chain Cϵ2 proton in the native complex does stabilize the carboxamide−main chain hydrogen bonds by ∼0.5 kcal/mol. However, the additional crowding of the carboxamide oxygen and its hydrogen bond donor by the larger indole ring in the Trp^{93} mutant destabilizes the nicotinamide end of the NAD complex by ∼2.3 kcal/mol.

As noted above, the nicotinamide carboxamide hydrogen bonds appear to be necessary for maintaining the catalytically active, closed form of the enzyme. Interference with these carboxamide−enzyme interactions by the Phe^{93} → Trp substitution may hinder formation of the closed conformation in the double mutant. Observation of an open conformation in the second double mutant complex discussed below supports this hypothesis.

General Features of NAD Cofactor Binding. As observed in other complexes, the adenine ring forms hydrophobic contacts with Ile^{224} and Ile^{269} and the adenine ribose hydroxyl groups forms hydrogen bonds with Asp^{223} and Lys^{228}. NAD torsion angles in the phosphate region show some variability between monomers, with associated variability in water-mediated contacts with the adenine phosphate oxygen O2PA. Polar interactions between Arg^{369} and the nicotinamide phosphate oxygen O1PN are also lengthened relative to those observed in the native complex and the F93W mutant. However, most solvent-mediated interactions identified in other moderate- and high-resolution native complexes are preserved in the double mutant. These include solvent-mediated interactions between the NAD phosphate oxygens and residues 367, 368, 369, 201, and 204 (*13*, *33*).

Substrate Binding. The trifluoroethanol substrate analogue remains in the active site, coordinated to the zinc cation via its hydroxyl oxygen (Figure 3). The trifluoroethanol oxygen also forms a hydrogen bond to Ser^{48}, which in turn hydrogen bonds to the O2′ ribose hydroxyl oxygen of the cofactor (Figure 3). A hydrogen bond between the ribose O3′ and His^{51} completes the first links in a putative relay system for transport of the alcohol hydroxyl proton to solvent (*42*, *43*). These interactions are preserved in the active single mutant ternary complexes (*1*).

In the single V203A mutant, the trifluoroethanol substrate is displaced away from the cofactor, toward position 93 (Figure 2). Substrate displacement in the V203A/F93W double mutant is limited by the presence of the tryptophan at position 93. The larger tryptophan forms a hydrophobic "cap", blocking further movement of the substrate deeper into the alcohol binding pocket (Figure 3). The substrate is sandwiched between the side chains of Trp^{93} and Ser^{48}, resulting in an apparent hydrogen bond interaction between one trifluoroethanol fluorine and the hydroxyl oxygen of Ser^{48}. The same effect is observed in the single F93W mutant (*1*).

V203A/F93W−CPAD

The complex between the V203A/F93W double mutant and NAD, described above, crystallizes in the closed conformation required for hydride transfer. However, the F93W mutation may destabilize this catalytically active conformation by sterically interfering with formation of a necessary enzyme−cofactor interaction.

Evidence for this hypothesis is offered by examination of the crystal structure of the V203A/F93W double mutant with a second ligand, the NAD analogue CPAD (Chart 1). CPAD is a nearly isosteric analogue of NAD in which the pyridinium group is replaced by a neutral pyridine ring (*10*). The two ligands are otherwise identical:

Chart 1: NAD Analogue CPAD

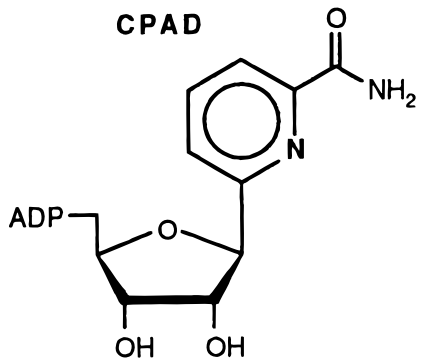

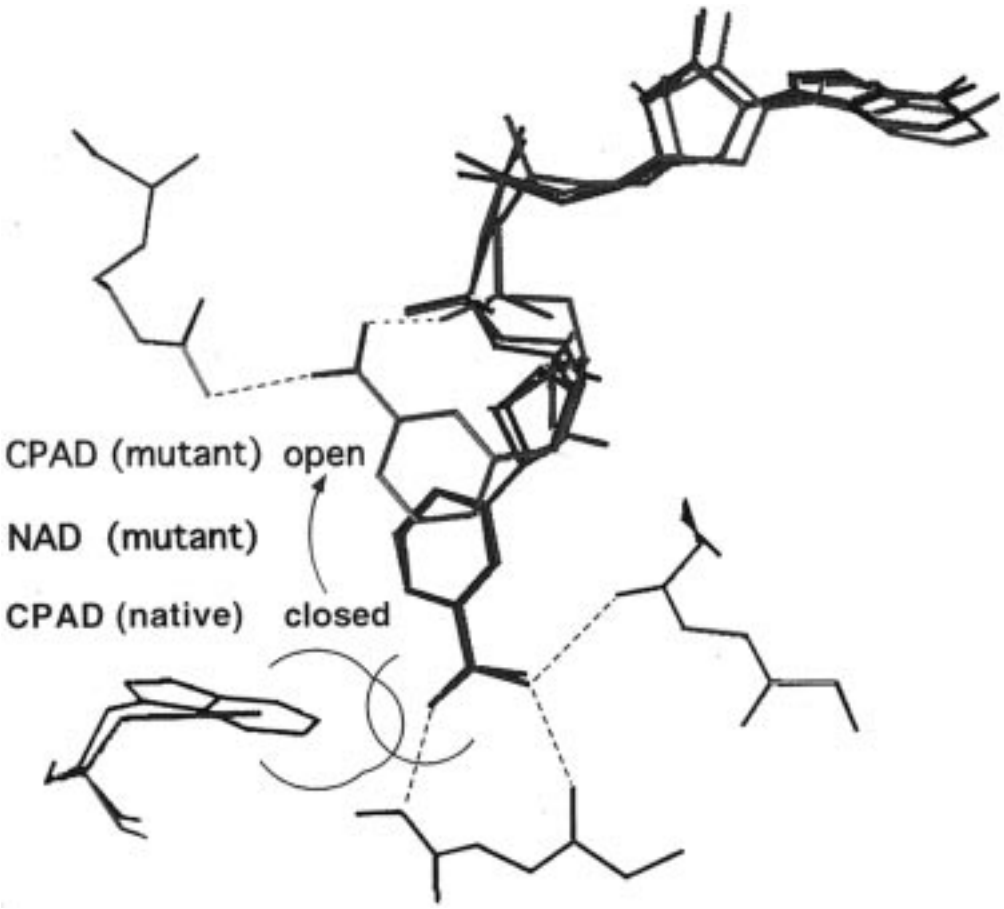

FIGURE 4: Comparison of active site residues and ligands in native and double mutant complexes with NAD or the isosteric analogue CPAD. CPAD bound to native LADH (green) closely mimics the conformation of NAD bound to closed-form native LADH (not shown) and the conformation of NAD bound to the closed-form double mutant F93W/V203A (magenta). In the closed F93W/V203A−NAD complex (magenta), unfavorable steric contacts occur between the NAD carboxamide group and mutated residue Trp^{93} (magenta van der Waals surfaces). These contacts are relieved in the F93W/V203A−CPAD complex (cyan) by rotation of the pyridine ring to a syn conformation (arrow). Loss of carboxamide hydrogen bonds to main chain atoms of residues 317, 319, and 292 (magenta dashed lines) results in an open complex. These are replaced by carboxamide hydrogen bonds to Arg^{369} and a phosphate oxygen (cyan dashed lines).

The complex between CPAD and the V203A/F93W double mutant crystallizes in the open conformation characteristic of the apoenzyme. The rms fit between backbone atoms of the double mutant in this complex and those of the native enzyme in its open conformation is 0.42 Å. However, the complex between CPAD and the native enzyme crystallizes in the closed form (*23*). The conformation of the CPAD ligand in the native complex very closely mimics the catalytically active geometry of NAD observed in other closed-form ternary complexes (*23*). This suggests that the failure of the ligand to stabilize a closed F93W/V203A complex is due in part to the double mutation.

CPAD Cofactor Binding and the Active Site. The conformation of the bound cofactor analogue in the open V203A/F93W complex is unusual and instructive. The most striking feature of the bound ligand is that the pyridine base swings from an anti conformation in the native enzyme to a syn conformation in the double mutant (Figure 1B). A comparison of the CPAD structures in the wild type, closed complex and the mutant, open complex is shown in Figure 4.

In all closed complexes, the nicotinamide or analogous base adopts an anti conformation relative to the ribose sugar. This allows formation of the three carboxamide hydrogen bonds to the main chain atoms of residues Val^{292}, Ala^{317}, and Phe^{319}. As discussed above, these hydrogen bonds may be required to maintain the closed conformation of the enzyme. Analogues lacking the nicotinamide moiety (*32*) or the carboxamide group (*37*) or otherwise constrained from adopting the required conformation (*22*, *26*) crystallize in the open form.

In the closed F93W−NAD complex (*1*), and the V203A/F93W−NAD complex described above, the cofactor nicotinamide ring is in the anti conformation, allowing its carboxamide substituent to maintain the hydrogen bonds required to stabilize the closed conformation (Figure 4). However, replacement of Phe^{93} by the larger tryptophan side chain in both of these closed mutant complexes results in an unfavorable steric contact with the carboxamide oxygen. This contact is relieved in the open V203A/F93W− CPAD complex by rotation of the base and carboxamide group away from Trp^{93} (Figure 4). The resulting syn conformation constitutes a 155° rotation relative to the anti conformation seen in the closed structures.

The question arises as to why the syn conformation is not observed in the V203A/F93W− NAD complex, which crystallizes in the closed form. NAD and CPAD, although isosteric, are not identical, differing in both the charge and position of the heterocycle anchoring the carboxamide group. Subtle differences in ligand binding at the active site are

sufficient to shift the equilibrum between open and closed forms of the enzyme in the crystallization medium (*28*). Results from ab initio calculations on a closed CPAD model complex are similar to those obtained for the NAD model (above); the close proximity of the Trp^{93} indole ring destabilizes the CPAD carboxamide−main chain interactions. Interestingly, these interactions are destabilized by ~3.2 kcal/mol in the CPAD model, an energy ~1 kcal/mol higher than that computed for the NAD complex (above).

In solution, it is likely that the V203A/F93W mutation allows some degree of NAD binding in a syn conformation similar to that observed for CPAD. A comparable effect is seen in the analogous L203A mutant of yeast alcohol dehydrogenase,[2] where an increase in B-side specific hydride transfers is also attributed to enhanced binding of NAD in the syn conformation (*44*). Stereospecificity of hydride transfer was not examined in the F93W/V203A LADH mutant. However, given the inability of the syn conformation to stabilize the closed form, the relative rate of hydride transfer to NAD in this alternative conformation is likely to be quite low, as is the case in the yeast enzyme (*44*).

In the open CPAD−mutant complex, the CPAD pyridine ring is stabilized in the syn conformation by carboxamide interactions different from those required to maintain closed complexes. In this open complex, the carboxamide carbonyl oxygen forms a hydrogen bond with a terminal amino group of Arg^{369} (Figure 4). As a result, the carboxamide amide nitrogen forms an intramolecular contact with a phosphate oxygen (not shown).

The syn ligand conformation observed here is similar to that seen in a complex between native LADH, NADH, and the inhibitor imidazole (*26*). In this structure, the dihydronicotinamide ring also adopts a syn conformation, the imidazole ligand having an effect analogous to that of the F93W mutation. The zinc-bound imidazole sterically prevents the nicotinamide ring from adopting the anti conformation required for closure of the enzyme. As a result, the three carboxamide hydrogen bonds are not maintained, and the complex crystallizes in the open form (*26*).

Alternative carboxamide interactions are also observed in the NADH−imidazole complex, although the carboxamide group is rotated by ~180° relative to the position modeled here (*26*). In the CPAD structure, ab initio calculations indicate that the carboxamide group clearly favors the conformation in which the amide nitrogen is adjacent to the pyridine nitrogen (see Experimental Procedures).

Comparison of the imidazole and CPAD complexes suggests that the second V203A mutation also facilitates cofactor binding in the syn conformation. The A side of the dihydronicotinamide ring in the native imidazole complex forms van der Waals contacts with the side chain of Val^{203} (*26*). Substitution by the smaller alanine at position 203 allows the ligand to bind more deeply in the interdomain cleft, with the pyridine ring forming van der Waals contacts with the methyl group of Ala^{203}, and the pyridine ribose forming contacts with the side chains of residue 293 and 268. Removal of the steric bulk of the valine methyl groups at position 203 may also provide the cofactor with additional freedom to rotate about the C-glycosidic bond into the syn conformation and account for the increased mobility seen in this conformer (see Experimental Procedures).

General Features of CPAD Binding. Interactions with the adenosine end of the CPAD ligand in the double mutant are similar to those seen in both open and closed complexes of the native enzyme and NADH. The adenine ring forms hydrophobic van der Waals contacts with the side chains of Ile^{224} and Ile^{269}. Asp^{223} forms hydrogen bonds with both adenine ribose hydroxyl oxygens O2′A and O3′A, and Lys^{228} donates a hydrogen bond to O3′A.

The pyrophosphate region of the ligand molecule binds in the interdomain cleft. In the open conformation of the protein, this cleft is comparatively wide, allowing significant positional freedom for the phosphate bridge. This was a region of high thermal factors and relatively poor definition in our electron density, indicating possible positional disorder. Hydrogen bonds are observed between the pyrophosphate oxygen O2PN and the main chain oxygen of Val^{268}. van der Waals contacts for the pyrophosphate bridge are provided by Gly^{201}, Ala^{203}, and Val^{268}.

The pyridine ribose hydroxyl oxygen O3′N forms a hydrogen bond with the main chain oxygen of Ile^{269}. This same interaction is found in both the closed NADH complex and the open ADPR complex (*32*). O2′N forms a long (3.2 Å) water-mediated interaction with both the main chain and a side chain oxygen of Glu^{267}. A second interaction is observed with the main chain oxygen of Gly^{293}.

DISCUSSION

The V203A/F93W double mutant LADH shows a 75-fold reduction in catalytic efficiency relative to that of the native enzyme, and reduced tunneling relative to that of either the V203A or F93W single mutant (*1*). The structures of the two double mutant V203A/F93W complexes described above and the two single mutant complexes described previously (*1*) suggest that perturbations in both ground state catalytic geometry and interdomain motion may influence catalytic efficiency and hydride tunneling. Several mechanisms may act in concert.

Closed structures of both the V203A− and V203A/F93W−NAD complexes consistently demonstrate displacement of the cofactor nicotinamide ring away from substrate, toward the gap left by removal of the bulky hydrophobic side chain at position 203 (Figure 2). This increases the distance between hydride donor and acceptor atoms in the closed complexes relative to that observed in the native enzyme (*1*). This alteration in ground state catalytic geometry is consistent with the reduced catalytic efficiency and tunneling observed in the V203A mutants. Even very small increases in barrier width can significantly decrease tunneling probability (*8*, *9*).

The increase in distance between C1 of alcohol and C4 of the nicotinamide ring in V203A/F93W (~0.4 Å) is approximately half of that observed in the single mutant V203A (~0.8 Å) (*1*). Thus, the double mutant would be expected to show greater tunneling, on the basis of distance (i.e., ground state) considerations alone. Clearly, other factors contribute to the reduced tunneling observed in the double mutant.

Addition of steric bulk at position 93 in the F93W mutants may also destabilize one of the three adjacent carboxamide−

[2] Using LADH numbering.

enzyme hydrogen bonds required to preserve the closed active conformation. Both the F93W− and V203A/F93W−NAD complexes show close steric contacts between the large Trp^{93} residue, the nicotinamide carboxamide oxygen, and its main chain amide proton donor of residue 317 (Figure 3). Ab initio calculations indicate that these contacts destabilize the backbone−carboxamide bond. This is apparently not a severe limitation in the F93W single mutant, which maintains a catalytic efficiency approximately half that of the wild type enzyme. Although hydrogen tunneling in F93W is more pronounced than that observed in all but one of the active site mutants examined, it is very likely reduced relative to that in the native enzyme (*7*).

In the V203A/F93W double mutant, the removal of steric bulk at position 203 may also allow the nicotinamide end of the cofactor increased flexibility in adopting an alternative syn conformation. A similar effect is observed kinetically in the L203A mutant of the homologous yeast enzyme[2] (*44*). In the LADH double mutant, the syn conformation additionally removes the Trp^{93}-induced crowding of the carboxamide oxygen, and this conformation is observed in the V203A/F93W−CPAD complex (Figure 4). However, the loss of the carboxamide−main chain hydrogen bonds in the syn ligand also results in an open, inactive enzyme conformation. A shift in the relative populations of open and closed forms of V203A/F93W in solution may contribute to the reduced activity seen in the double mutant.

Last, the F93W mutation potentially hinders hyperclosure of the enzyme, which in turn may reduce hydride tunneling. The hyperclosed conformation was first observed in the V203A single mutant (*1*). It is characterized by reduced crystal solvent content and a narrowed interdomain cleft relative to that seen in other closed complexes. Narrowing of the interdomain cleft in the hyperclosed V203A mutant results from an approximately 0.5 Å rigid body shift of the catalytic domain toward the cofactor domain. This further decreases the distance between the NAD carboxamide oxygen and the phenyl group at position 93 (*1*). Replacement of Phe^{93} with the bulkier tryptophan in the hyperclosed conformation would create steric interactions with the carboxamide group even closer than those already observed in the closed F93W and F93W/V203A structures. This would disrupt the carboxamide−main chain hydrogen bonds and likely destabilize the closed conformation altogether. The failure to observe hyperclosure in either the single F93W mutant (*1*) or the double V203A/F93W mutants supports this hypothesis.

We have recently observed similar low-solvent hyperclosed conformations in two native LADH ternary complexes, indicating that an interdomain mutation is not required for this effect.[3] The hyperclosed geometry illustrates the flexibility in interdomain motion available to LADH, even in an active closed ternary complex. This interdomain flexibility may be used in the native enzyme to transiently narrow the hydride donor−acceptor distance, increase tunneling probability, and optimize catalysis (*8*, *9*). However, vibrationally induced hyperclosure of the enzyme would be inhibited by the F93W mutation, which appears to be sterically incompatible with further narrowing of the interdomain cleft (above).

Thus, the V203A/F93W double mutation potentially (a) destabilizes formation of the closed conformation of the enzyme, (b) perturbs the catalytic geometry in the closed conformation, and (c) inhibits vibrationally induced enhancement of catalysis. The double mutant shows a 75-fold reduction in catalytic efficiency relative to that of the native enzyme, and reduced tunneling relative to that of either single mutant (*1*). Mutations at the domain interface clearly produce subtle changes in the static ground state catalytic geometry, and may perturb the dynamic behavior of the enzyme as well. Additional studies will test these hypotheses.

[3] These complexes contain isosteric NAD analogues benzamide adenine dinucleotide and thiazole-4-carboxamide adenine dinucleotide, respectively (B. Goldstein, unpublished data).

ACKNOWLEDGMENT

We are indebted to Drs. Krzystof W. Pankiewicz and Kyoichi A. Watanabe (Codon Pharmaceuticals, Gaithersburg, MD) for CPAD, to Prof. Bryce V. Plapp (University of Iowa, Iowa City, IA) for the plasmid containing the gene for LADH, and to Drs. H. L. Carrell and J. P. Glusker (Fox Chase Cancer Center, Fox Chase, PA) for use of their diffraction facility with the CPAD complex.

SUPPORTING INFORMATION AVAILABLE

Ramachandran plots for the V203A−NAD and V203A−CPAD complexes (5 pages). Ordering information is given on any current masthead page.

REFERENCES

1. Bahnson, B. J., Colby, T. D., Chin, J. K., Goldstein, B. M., and Klinman, J. P. (1997) *Proc. Natl. Acad. Sci. U.S.A. 94*, 12797−802.
2. Eklund, H., and Brändén, C.-I. (1987) in *Biological Macromolecules and Assemblies. Volume 3: Active Sites of Enzymes* (Jurnak, F. A., and McPherson, A., Eds.) pp 74−142, John Wiley & Sons, New York.
3. Eklund, H. (1989) *Biochem. Soc. Trans. 17*, 293−6.
4. Sekhar, V. C., and Plapp, B. V. (1988) *Biochemistry 27*, 5082−8.
5. Sekhar, V. C., and Plapp, B. V. (1990) *Biochemistry 29*, 4289−95.
6. Cha, Y., Murray, C. J., and Klinman, J. P. (1989) *Science 243*, 1325−30.
7. Bahnson, B. J., Park, D.-H., Kim, K., Plapp, B. V., and Klinman, J. P. (1993) *Biochemistry 32*, 5503−7.
8. Rodgers, J., Femec, D. A., and Schowen, R. L. (1982) *J. Am. Chem. Soc. 104*, 3263−8.
9. Bruno, W. J., and Bialek, W. (1992) *Biophys. J. 63*, 689−99.
10. Pankiewicz, K. W., Zeidler, J., Ciszewski, L. A., Bell, J. E., Goldstein, B. M., Jayaram, H. N., and Watanabe, K. A. (1993) *J. Med. Chem. 36*, 1855−9.
11. Rodgers, D. W. (1997) *Methods Enzymol. 276*, 183−203.
12. Otwinowski, Z., and Minor, W. (1997) *Methods Enzymol. 276*, 307−26.
13. Al-Karadaghi, S., Cedergren-Zeppezauer, E. S., Hövmoller, S., Petratos, K., Terry, H., and Wilson, K. S. (1994) *Acta Crystallogr. D50*, 793−807.
14. Brünger, A. T. (1992) *X-PLOR Version 3.1. A System for X-ray Crystallography and NMR*, Yale University Press, New Haven, CT.
15. Engh, R. A., and Huber, R. (1991) *Acta Crystallogr. A47*, 392−400.
16. Sack, J. S. (1988) *J. Mol. Graphics 6*, 224−5.

17. Brünger, A. T. (1992) *Nature 355*, 472−5.
18. Brünger, A. T., Krukowski, A., and Erickson, J. W. (1990) *Acta Crystallogr. A46*, 585−93.
19. Kabsch, W. (1988) *J. Appl. Crystallogr. 21*, 916−24.
20. Kabsch, W. (1988) *J. Appl. Crystallogr. 21*, 67−71.
21. Eklund, H., Nordstrom, B., Zeppezauer, E., Soderlund, G., Ohlsson, I., Boiwe, T., Soderberg, B. O., Tapia, O., Brändén, C.-I., and Åkeson, A. (1976) *J. Mol. Biol. 102*, 27−59.
22. Li, H., Hallows, W. H., Punzi, J. S., Marquez, V. E., Carrell, H. L., Pankiewicz, K. W., Watanabe, K. A., and Goldstein, B. M. (1994) *Biochemistry 33*, 23−32.
23. Li, H., Hallows, W. H., Punzi, J. S., Pankiewicz, K. W., Watanabe, K. A., and Goldstein, B. M. (1994) *Biochemistry 33*, 11734−44.
24. Frisch, M. J., Trucks, G. W., Head-Gordon, M., Gill, P. M. W., Wong, M. W., Foresman, J. B., Johnson, B. G., Schlege, l. H. B., Robb, M. A., Replogle, E. S., Gomperts, R., Andres, J. L., Raghavachari, K., Binkley, J. S., Gonzalez, C., Martin, R. L., Fox, D. J., Defrees, D. J., Baker, J., Stewart, J. J. P., and Pople, J. A. (1992) *Gaussian92*, Gaussian, Inc., Pittsburgh, PA.
25. Li, H., and Goldstein, B. M. (1992) *J. Med. Chem. 35*, 3560−7.
26. Cedergren-Zeppezauer, E. (1983) *Biochemistry 22*, 5761−72.
27. Hodel, A., Kim, S. H., and Brünger, A. T. (1992) *Acta Crystallogr. A48*, 851−8.
28. Cedergren-Zeppezauer, E., Samama, J.-P., and Eklund, H. (1982) *Biochemistry 21*, 4895−908.
29. Frisch, M. J., Trucks, G. W., Schlegel, H. B., Gill, P. M. W., Johnson, B. G., Robb, M. A., Cheeseman, J. R., Keith, T., Petersson, G. A., Montgomery, J. A., Raghavachari, K., Al-Laham, M. A., Zakrzewski, V. G., Ortiz, J. V., Foresman, J. B., Cioslowski, J., Stefanov, B. B., Nanayakkara, A., Challacombe, M., Peng, C. Y., Ayala, P. Y., Chen, W., Wong, M. W., Andres, J. L., Replogle, E. S., Gomperts, R., Martin, R. L., Fox, D. J., Binkley, J. S., Defrees, D. J., Baker, J., Stewart, J. P., Head-Gordon, M., Gonzalez, C., and Pople, J. A. (1995) *Gaussian94*, Gaussian, Inc., Pittsburgh, PA.
30. Frisch, M. J., Frisch, E., and Forseman, J. B. (1995) *Gaussian 94 User's Reference, Version 5*, Gaussian, Inc., Pittsburgh, PA.
31. Hehre, W. J., Radom, L., Schleyer, P. v. R., and Pople, J. A. (1986) *Ab Initio Molecular Orbital Theory*, John Wiley & Sons, New York.
32. Eklund, H., Samama, J.-P., and Jones, T. A. (1984) *Biochemistry 23*, 5982−96.
33. Ramaswamy, S., Eklund, H., and Plapp, B. V. (1994) *Biochemistry 33*, 5230−7.
34. Ramaswamy, S., Scholze, M., and Plapp, B. V. (1997) *Biochemistry 36*, 3522−7.
35. Cho, H., Ramaswamy, S., and Plapp, B. V. (1997) *Biochemistry 36*, 382−9.
36. Eklund, H., Samama, J.-P., and Wallen, L. (1982) *Biochemistry 21*, 4858−66.
37. Samama, J. P., Zeppezauer, E., Biellmann, J. F., and Brändén, C.-I. (1977) *Eur. J. Biochem. 81*, 403−9.
38. Gould, R. O., Gray, A. M., Taylor, P., and Walkinshaw, M. D. (1985) *J. Am. Chem. Soc. 107*, 5921−7.
39. Thomas, K. A., Smith, G. M., Thomas, T. B., and Feldmann, R. J. (1982) *Proc. Natl. Acad. Sci. U.S.A. 79*, 4843−7.
40. Burley, S. K., and Petsko, G. A. (1988) *Adv. Protein Chem. 39*, 125−89.
41. Auld, D. S., Young, G. B., Saunders, A. J., Doyle, D. F., Betz, S. F., and Pielak, G. J. (1993) *Protein Sci. 2*, 2187−97.
42. Eklund, H., Plapp, B. V., Samama, J.-P., and Brändén, C.-I. (1982) *J. Biol. Chem. 257*, 14349−58.
43. Hennecke, M., and Plapp, B. V. (1983) *Biochemistry 22*, 3721−8.
44. Weinhold, E. G., Glasfeld, A., Ellington, A. D., and Benner, S. A. (1991) *Proc. Natl. Acad. Sci. U.S.A. 88*, 8420−4.

BI973184B